The Journal of Immunology

Importance of Endosomal Cathelicidin Degradation To Enhance DNA-Induced Chicken Macrophage Activation

Maarten Coorens, Albert van Dijk, Floris Bikker, Edwin J. A. Veldhuizen and Henk P. Haagsman

J Immunol 2015; 195:3970-3977; Prepublished online 16 September 2015;
doi: 10.4049/jimmunol.1501242
http://www.jimmunol.org/content/195/8/3970

The Journal of Immunology is published twice each month by
The American Association of Immunologists, Inc.,
9650 Rockville Pike, Bethesda, MD 20814-3994.

Print ISSN: 0022-1767 Online ISSN: 1550-6606.

Importance of Endosomal Cathelicidin Degradation To Enhance DNA-Induced Chicken Macrophage Activation

Maarten Coorens,* Albert van Dijk,* Floris Bikker,† Edwin J. A. Veldhuizen,* and Henk P. Haagsman*

Cathelicidins are essential in the protection against invading pathogens through both their direct antimicrobial activity and their immunomodulatory functions. Although cathelicidins are known to modulate activation by several TLR ligands, little is known about their influence on DNA-induced macrophage activation. In this study, we explored the effects of cathelicidins on DNA-induced activation of chicken macrophages and elucidated the intracellular processes underlying these effects. Our results show that chicken cathelicidin (CATH)-2 strongly enhances DNA-induced activation of both chicken and mammalian macrophages because of enhanced endocytosis of DNA–CATH-2 complexes. After endocytosis, DNA is liberated from the complex because of proteolytic breakdown of CATH-2, after which TLR21 is activated. This leads to increased cytokine expression and NO production. Through the interaction with DNA, CATH-2 can play an important role in modulating the immune response at sites of infection. These observations underline the importance of cathelicidins in sensing bacterial products and regulating immune responses. ***The Journal of Immunology*****, 2015, 195: 3970–3977.**

Host defense peptides (HDPs) are a group of short cationic peptides with an essential role in the innate host defense system (1). HDPs, which are also known as antimicrobial peptides, are mainly produced by leukocytes and epithelial cells at sites of infection and/or mucosal surfaces (2). They are known for their broad-spectrum antimicrobial activity and their more recently discovered immunomodulatory functions (3). Their importance in innate host defense has been clearly demonstrated in several in vivo knockout models, where loss of HDP expression was shown to result in an increased susceptibility to infections (4–6). In addition, administration of HDPs was shown to have a protective effect in multiple in vivo infection models (7–9). Because of this strong protective activity, therapeutic use of HDPs as anti-infectives has gained great interest in both human and veterinary medicine (10).

Another important molecule in the regulation of infection and inflammation is extracellular DNA. During infections, DNA is released from various sources into the extracellular microenvironment and subsequently activates DNA receptors to induce immune activation (11). Bacteria secrete DNA during biofilm formation (12) or can release DNA after being killed by antimicrobial components (13, 14). Host cells either secrete DNA actively, that is, neutrophils undergoing NETosis (15), or release DNA passively, due to tissue damage (16). Moreover, administration of synthetic DNA is often used during vaccination therapies to boost vaccination efficiency (17). Interestingly, the potential of extracellular DNA to induce an inflammatory response depends greatly on other extracellular components, such as HDPs. For example, in psoriasis patients, complex formation between HDPs and DNA has been shown to induce a strong inflammatory response by enhancing DNA uptake in plasmacytoid dendritic cells (pDCs). This subsequently increases TLR9 activation, which leads to more IFN-α production (18–20). Although these articles show the strong potential of HDPs in regulating DNA-induced immune activation, little is known about the role of HDPs in DNA-induced activation in other cell types, such as macrophages.

In this study, we focused on elucidating the role of cathelicidins in chicken innate immune activation by extracellular DNA. This has led to the identification of chicken cathelicidin (CATH)-2 as a potent enhancer of DNA-induced macrophage activation in both avian and mammalian macrophages. Enhancement of DNA-induced activation results from enhanced DNA–CATH-2 complex endocytosis and subsequent TLR21 activation. The endosomal degradation of CATH-2, which releases the DNA from the complex and enables it to activate TLR21, was found to be essential in this process. Ultimately, this leads to the amplification of DNA-inducible macrophage responses, such as cytokine expression and NO production.

Elucidation of the role of CATH-2 in DNA-induced macrophage activation provides new insight in both the evolutionary conservation of cathelicidin functions and the role of cathelicidins in innate immunity. Moreover, these results provide useful information for the development of multifunctional HDP-based anti-infective therapies.

*Division of Molecular Host Defence, Faculty of Veterinary Medicine, Department of Infectious Diseases and Immunology, Utrecht University, 3584 CL Utrecht, the Netherlands; and †Department of Oral Biochemistry, Academic Centre for Dentistry Amsterdam, University of Amsterdam and VU University Amsterdam, 1081 LA Amsterdam, the Netherlands

ORCID: 0000-0002-4931-5201 (H.P.H.).

Received for publication June 3, 2015. Accepted for publication August 12, 2015.

This work was supported by the Immuno Valley ALTernatives to ANTibiotics (ALTANT) Animal Specific Immuno-modulatory Antimicrobials (ASIA) 2 program of the Dutch Ministry of Economic Affairs.

M.C., A.v.D., and H.P.H. designed research; M.C. performed research; F.B. provided custom synthetic peptides; M.C., F.B., A.v.D., E.J.A.V., and H.P.H. analyzed data; and M.C. wrote the paper.

Address correspondence and reprint requests to Prof. Henk P. Haagsman, Division of Molecular Host Defence, Faculty of Veterinary Medicine, Department of Infectious Diseases and Immunology, Utrecht University, Yalelaan 1, 3584 CL Utrecht, the Netherlands. E-mail address: H.P.Haagsman@uu.nl

The online version of this article contains supplemental material.

Abbreviations used in this article: AF488, Alexa Fluor 488; CATH, chicken cathelicidin; DNA-AF488, 3′-labeled ODN-2006-Alexa Fluor 488; EIPA, 5-(N-Ethyl-N-isopropyl)amiloride; HDP, host defense peptide; ITC, isothermal titration calorimetry; ODN, oligodeoxynucleotide; pDC, plasmacytoid dendritic cell; qPCR, quantitative PCR; RT, room temperature.

www.jimmunol.org/cgi/doi/10.4049/jimmunol.1501242

Materials and Methods

Reagents and stimulation

CATH-2 (21) and D-CATH-2 were synthesized by Fmoc-chemistry (CPC Scientific, Sunnyvale, CA). Truncated peptides (Table I) and N-terminal labeled peptides, as well as LL-37 and CRAMP, were synthesized by Fmoc-chemistry at the Academic Centre for Dentistry Amsterdam (Amsterdam, the Netherlands). Oligodeoxynucleotide (ODN)-1826, ODN-2216, ODN-2006, ODN-M362, inhibitory ODN (ODN-TTAGGG), control ODN (ODN-2088 control), *E. coli* DNA, and *S. minnesota* LPS were obtained from Invivogen (Toulouse, France). 3′-Labeled ODN-2006-Alexa Fluor 488 (DNA-AF488) and ODN-2006 for isothermal titration calorimetry (ITC) experiments were obtained from Eurofins MWG Operon (Huntsville, AL). Endocytosis inhibitors chlorpromazine, 5-(N-Ethyl-N-isopropyl)amiloride (EIPA), cytochalasin B, methyl-β-cyclodextrin, filipin, and nocodazole were obtained from Sigma Aldrich (St. Louis, MO). Endosome acidification inhibitors that were used are chloroquine (Sigma Aldrich), bafilomycin A1 (Invivogen), and NH_4Cl (Merck, Kenilworth, NJ). All experiments described concerning DNA and peptide stimulation were performed by premixing the DNA and the peptide of interest in culture medium, followed immediately by stimulation of cells with this mixture.

Cell cultures

Chicken macrophage cell lines HD11 (22) and MQ-NCSU (23), as well as murine macrophage cell line RAW264.7 (24), were a kind gift from Prof. Jos van Putten, Utrecht University (Utrecht, the Netherlands). HD11 cells were cultured in RPMI 1640 (Life Technologies, Carlsbad, CA) complemented with 10% FBS (GE Healthcare Europe GmbH, Eindhoven, the Netherlands), MQ-NCSU cells were cultured in DMEM (Life Technologies) complemented with 10% FBS and 1% nonessential amino acids (Life Technologies), and RAW264.7 cells were cultured in DMEM complemented with 10% FBS. All cell lines were kept at 37°C, 5.0% CO_2. Chicken PBMCs were obtained from healthy adult chickens. Blood was diluted in PBS, and blood cells were separated by Ficoll density gradient centrifugation. PBMCs were collected at the interphase and washed with RPMI 1640. For primary monocyte selection, PBMCs were seeded at 1×10^7 cells/well in a 48-well plate in RPMI 1640 complemented with 10% FBS and 1% penicillin/streptomycin (Life Technologies). After overnight adherence at 41°C, 5.0% CO_2, cells were washed three times with RPMI 1640 and incubated with fresh RPMI 1640 complemented with 10% FBS and 1% penicillin/streptomycin. After an additional 3-d incubation, cells were used for stimulation.

Inhibition assays

Endocytosis inhibition assays were performed by preincubation for 1 h with chlorpromazine (30 μM), EIPA (80 μM), cytochalasin B (10 μM), methyl-β-cyclodextrin (5 mM), filipin (2 μg/ml), or nocodazole (20 μM) and subsequent coincubation with inhibitors and stimulants for 4 h. Viability was assessed by the WST-1 assay (Roche, Basel, Switzerland) following manufacturer's protocol. For endosome acidification inhibition, chloroquine (25 μg/ml), bafilomycin A1 (250 nM), or NH_4Cl (10 mM) was used during stimulation. For inhibition of TLR21, cells were preincubated for 5 h with inhibitory ODN (ODN-TTAGGG) or control ODN (2 μM). After preincubation, cells were washed and treated with indicated stimulants.

Griess assay

NO production was measured by the Griess Assay. A total of 5×10^4 HD11 cells were seeded in a 96-well plate and incubated overnight. After 17-h stimulation, 50 μl supernatant was mixed with 50 μl 1% sulfanilamide (5% phosphoric acid) and incubated 5 min at room temperature (RT) in the dark. A total of 50 μl 0.1% *N*-(1-naphthyl)ethylenediamine dihydrochloride was added before another 5-min incubation at RT in the dark. Absorbance was measured at 550 nm. For stimulation with *E. coli* DNA, DNA was diluted in incubation buffer (1 M NaCl, 20 mM Tris, 2 mM $MnCl_2$) and treated with DNase I (Roche) for 0, 1, or 2 min. DNAse activity was stopped with inhibition buffer (20 mM Tris, 8 mM EDTA), and DNA length was determined by gel electrophoresis.

TNF-α ELISA

For quantification of TNF-α production, 5×10^4 RAW 264.7 cells were seeded in a 96-well plate and incubated overnight. Cells were stimulated for 24 h, after which supernatant was collected and stored at −20°C. Samples were diluted 5× in 1% BSA in PBS pH 7.4. ELISAs were performed using the TNF-α ELISA DuoSet (R&D Systems, Minneapolis, MN) following the manufacturer's protocol.

Quantitative PCR

For quantitative PCR (qPCR) experiments, cells were stimulated for 4 h, after which RNA was isolated with the High Pure RNA Tissue kit (Roche). RNA was converted to cDNA using iScript cDNA synthesis kit (Bio-Rad, Veenendaal, the Netherlands). qPCR was performed using primers, probes (Supplemental Table I), and IQ supermix (Bio-Rad). Experiments were performed using CFX Connect qPCR with CFX Manager 3.0 (Bio-Rad). Quantification cycle values were corrected for PCR efficiency and housekeeping gene expression (28S and GAPDH). When no signal was detected after 40 cycles, samples were given an arbitrary quantification cycle value of 40. Unstimulated samples were set to 1.

Confocal microscopy

Experiments were performed with DNA-AF488. Cells were seeded at 4×10^4/well on 8-mm glass coverslips in a 48-well plate and incubated overnight. After 4-h stimulation with 25 nM DNA-AF488 with or without 5 μM peptide, cells were washed twice with RPMI 1640 and fixed in 4% paraformaldehyde in 0.1 M phosphate buffer (Na_2HPO_4 + KH_2PO_4), pH 7.4 for 30 min at RT. Cells were subsequently incubated with 20 mM NH_4Cl in PBS for 15 min at RT. Cells were washed once with PBS and stained with 1:500 WGA-Alexa Fluor 647 (Life Technologies) in PBS for 30 min. Cells were washed twice with PBS, once with H_2O, and mounted in FluoroSave (Merck Millipore, Billerica, MA) on a coverslide. Confocal imaging was performed on a Leica SPE-II DMI4000 microscope with LAS-AF software (Leica, Wetzlar, Germany) using a 100× HCX PLAN APO OIL CS objective. Z-stacks consist of 10 images taken over 1.17 μm. Averages of four frames per image were obtained at a resolution of 2048 × 2048. Image analysis was performed with ImageJ (National Institutes of Health, Bethesda, MD). Z-stacks were converted to average intensity images after which brightness and contrast were adjusted equally on all images.

Flow cytometry

Experiments were performed with DNA-AF488. HD11 cells were seeded at 3×10^5 in 24-well plates and incubated overnight. After 4-h stimulation, cells were washed twice with PBS, harvested mechanically with a cell scraper (Corning, Corning, NY) in PBS, and transferred to BD Falcon tubes. Cells were kept on ice in the dark and were analyzed immediately with a FACSCalibur (BD Biosciences, San Jose, CA). Data were analyzed using FlowJo software (FlowJo LLC, Ashland, OR).

Gel electrophoresis

For gel electrophoresis, ODN-2006 (1 μg, 8.7 μM) was incubated with various concentrations of peptide for 30 min at RT in RPMI 1640 medium + 10% FBS. After incubation, samples were run on a 1% agarose gel. DNA migration was visualized by staining the gel with Midori Green Advance DNA stain (Nippon Genetics Europe GmbH, Dueren, Germany) and analyzed with a ChemiDoc (Bio-Rad).

Isothermal titration calorimetry

ITC experiments were performed using the Low Volume NanoITC (TA Instruments–Waters LLC, New Castle, DE). The 50-μl syringe contained 200 μM peptide and the cell contained 250 μl 8 μM ODN-2006. Both peptide and ODN-2006 were diluted in the same 10 mM phosphate buffer (pH 7.4 or 4.4) containing Na_2HPO_4-KH_2PO_4 and 100 mM NaCl. Titrations were incremental with 1-μl injections at 300-s intervals. Experiments were performed at 37°C. Data were analyzed with the Nano Analyze software (TA Instruments–Waters LLC).

Statistical analysis and graphics

Statistical analysis was performed using SPSS 20 (IBM, Armonk, NY). Data were analyzed by independent samples *t* test for comparison of two groups or one-way ANOVA with Dunnett's post hoc test for more than two groups. Levene's test was used to determine homogeneity of variance. Pearson's correlation test was used to determine linear correlation. For qPCR analysis, data were log-transformed. Prism 5 software (GraphPad, La Jolla, CA) was used for graphical presentation of data.

Results

CATH-2 enhances DNA-induced macrophage activation

To determine the effect of cathelicidins on DNA-induced chicken macrophage activation, we stimulated HD11 cells with DNA in the form of a single-stranded ODN (ODN-2006), in the presence of

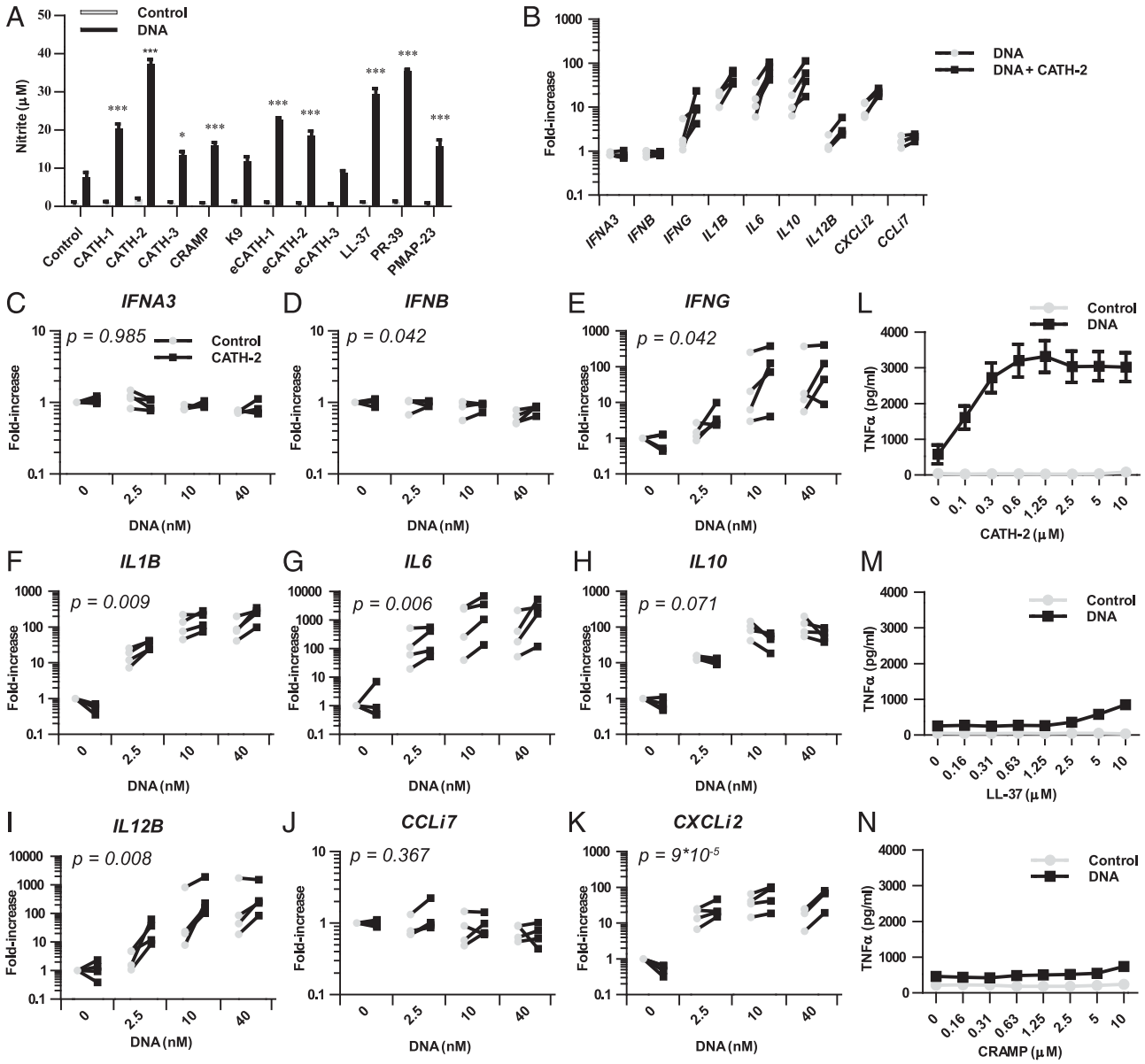

FIGURE 1. Enhancement of DNA-induced macrophage activation by cathelicidins. (**A**) NO production by HD11 cells with selected cathelicidins (5 μM) from different species in the presence or absence of 2.5 nM ODN-2006. The *p* values are obtained by one-way ANOVA with Dunnett's post hoc test (*$p < 0.05$, ***$p < 0.001$). $n = 3$; error bars = SEM. (**B**) qPCR analysis of cytokine expression after HD11 cell stimulation with 2.5 nM ODN-2006 in the presence or absence of CATH-2 (5 μM). Data represent fold-increase in cytokine expression normalized to unstimulated cells. $n = 4$. (**C**–**K**) Expression of (C) *IFNA3*, (D) *IFNB*, (E) *IFNG*, (F) *IL1B*, (G) *IL6*, (H) *IL10*, (I) *IL12B*, (J) *CCLi7*, and (K) *CXCLi2* in adherent monocytes, isolated from blood of four different chickens. Cells were stimulated with ODN-2006 in presence or absence of CATH-2 (5 μM). Data represent fold-increase in cytokine expression normalized to unstimulated cells. Two-way repeated-measures ANOVA was performed to determine significance of CATH-2 presence. $n = 4$. (**L**–**N**) TNF-α production of RAW264.7 macrophages after stimulation with 2.5 nM ODN-1826 in presence of different concentrations of (L) CATH-2, (M) LL-37 or (N) CRAMP. $n = 6$ for (L) and (M). $n = 3$ for (N). Error bars = SEM.

different chicken or mammalian cathelicidins (Fig. 1A). The three CATHs, CATH-1, -2, and -3, were all able to increase DNA-induced HD11 activation, as measured by means of NO production, with CATH-2 being the most potent. Other cathelicidins with known DNA-enhancing abilities, including human LL-37 (18), porcine PR-39 and PMAP-23 (25), and murine CRAMP (19), increased DNA-induced NO production as well. In addition, equine cathelicidin-1 and -2 also enhanced activation, whereas equine cathelicidin-3 and canine K9 did not significantly increase activation. Stimulation with cathelicidins only did not induce NO production. Because CATH-2 was the most potent cathelicidin to enhance the DNA-induced activation, this peptide was chosen to further determine the mechanism of enhancement of DNA-induced macrophage activation in more detail.

Thus, to further characterize the activation state of the HD11 cells, we determined gene expression of *IFNA3*, *IFNB*, *IFNG*, *IL1B*, *IL6*, *IL10*, *IL12B*, *CXCLi2*, and *CCLi7* after coincubation with DNA and CATH-2 (Fig. 1B, Supplemental Table II). Coincubation resulted in enhanced expression of multiple DNA-inducible genes, including *IL1B*, *IL6*, *CXCLi2*, *IL12B*, and *IFNG*. In addition, these genes were also slightly enhanced after stimulation with DNA and LL-37, although not significantly. Gene expression of *IFNA3*, *IFNB*, and *CCLi7* was unaffected by stimulation with DNA, cathelicidins, or a combination of both. To rule

out cell line–specific effects, we screened the chicken macrophage cell line MQ-NCSU (Supplemental Table II) and primary chicken monocytes (Fig. 1C–K) for cytokine expression. Coincubation of MQ-NCSU cells with DNA and CATH-2 resulted in a similar expression pattern compared with HD11 cells, whereas LL-37 was unable to enhance DNA-induced expression. In line with these results, stimulation of primary monocytes with DNA and CATH-2 resulted in enhanced expression of *IFNG, IL1B*, *IL6*, *IL12B*, and *CXCLi2*. DNA-induced expression of *IL10* in the presence of CATH-2 was slightly lower, albeit not significant. No changes were observed in expression of type I IFNs or *CCLi7* either.

Because mammalian cathelicidins were able to enhance DNA-induced NO production of chicken macrophages, CATH-2 was analyzed for possible cross-species activation. To test this, we stimulated murine RAW264.7 cells with DNA in combination with either CATH-2 (Fig. 1L), LL-37 (Fig. 1M), or CRAMP (Fig. 1N). Again, CATH-2 strongly enhanced DNA-induced activation, measured by TNF-α production. LL-37 augmented the activity as well, although not as potently as CATH-2, whereas CRAMP did not enhance activation. Taken together, these results indicate that of the peptides tested, CATH-2 is the most potent enhancer of DNA-induced macrophage activation in both avian and mammalian macrophages.

CATH-2 enhances both ssDNA and dsDNA activity

To determine whether CATH-2 could enhance macrophage activation by different DNA types, we incubated HD11 cells with different ODNs (Fig. 2A–D). ODN-2216 is an A-type ODN, which forms complex G-tetrad structures. ODN-2006 is a B-type ODN, which remains single-stranded, and ODN-M362 is a C-type ODN, which forms dimers (26). Stimulation with only cathelicidins (Fig. 2A) or ODN-2216 with or without cathelicidins (Fig. 2B) did not result in any NO production. Activation induced by ODN-2006 (Fig 2C, Supplemental Fig. 1A) and ODN-M362 (Fig. 2D) was clearly enhanced by CATH-2. ODN-2006– and ODN-M362–induced activation was also enhanced by LL-37, although higher concentrations of up to 5 μM LL-37 were needed to enhance the activation. In addition, CATH-2 was able to enhance activation of HD11 cells by *E. coli* DNA of different lengths (Fig. 2E, 2F).

Enhanced activation is dependent on increased DNA uptake

The ability of LL-37 to enhance DNA-induced activation in pDCs is dependent on complex formation between LL-37 and DNA (18). To verify whether complex formation occurs between CATH-2 and DNA, both components were mixed in RPMI 1640 medium supplemented with 10% FBS and run on an agarose gel. Migration of DNA was inhibited in the presence of either CATH-2 or LL-37 (Supplemental Fig. 1B), suggesting interaction between the two components. To further assess the interaction, we performed ITC analysis. ITC analysis confirmed high-affinity binding between DNA and both CATH-2 and LL-37, with K_d values of 11.3 nM (Supplemental Fig. 1C) and 110 nM (Supplemental Fig. 1D), respectively. In addition, the binding between CATH-2 and DNA was enthalpy driven ($\Delta H = -97.9$ kJ/mol) and showed a loss of entropy ($\Delta S = -163.4$ J/mol*K), which suggests strong ionic interaction between the cationic residues of the peptide and the anionic phosphate groups of the DNA backbone.

To determine whether the enhancement of DNA-induced activation is a result of increased DNA uptake, we stimulated HD11 cells with DNA-AF488 and CATH-2, after which DNA uptake was analyzed by confocal microscopy (Fig. 3A–D). Confocal images showed an increased uptake of DNA-AF488 in the presence of CATH-2 (Fig. 3C) compared with DNA-AF488 alone (Fig. 3B), with punctate intracellular localization of the DNA suggesting endosomal uptake. DNA uptake was enhanced to a lesser extent

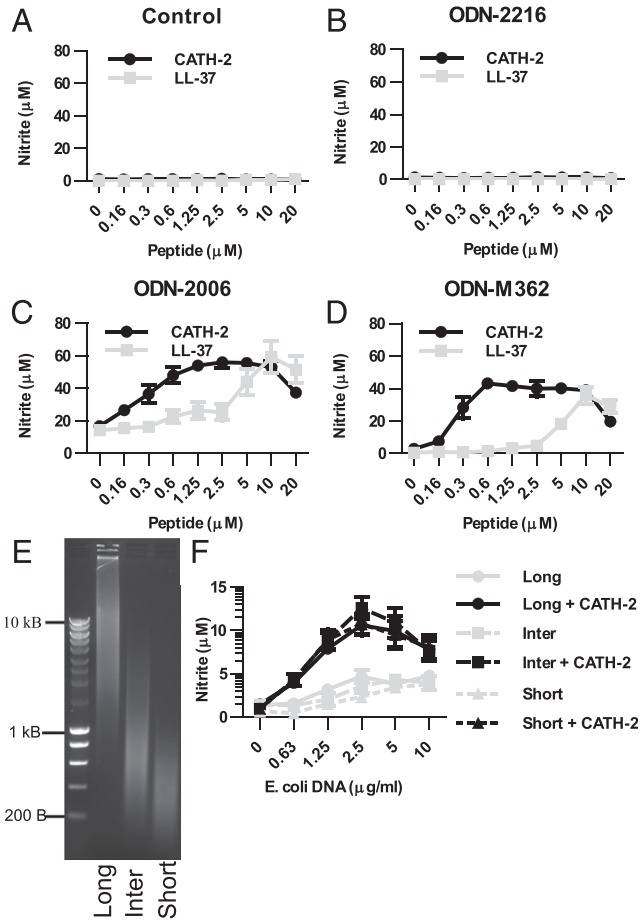

FIGURE 2. DNA-type specific enhancement of macrophage activation. NO production of HD11 cells stimulated with CATH-2 or LL-37 in (**A**) the absence of DNA or presence of 2.5 nM (**B**) ODN-2216, (**C**) ODN-2006, or (**D**) ODN-M362. n = 3–7; error bars = SEM. (**E**) Gel electrophoresis of *E. coli* DNA after 0, 1, or 2 min of DNAse I digestion. Samples were analyzed on 1% agarose gel. Representative of two independent experiments. (**F**) NO production of HD11 cells stimulated with *E. coli* DNA as digested in (E) presence or absence of CATH-2 (5 μM). n = 3. Error bars = SEM.

by LL-37 (Fig. 3D). Quantification of the uptake by flow cytometry (Fig. 3E) also confirmed the enhanced DNA uptake by CATH-2 and LL-37. Mouse cathelicidin CRAMP, however, did not significantly alter DNA uptake. To confirm whether CATH-2–enhanced DNA uptake correlates to the enhanced activation, we synthesized several truncated analogs of CATH-2 (Fig. 3F, Table I). Augmented DNA uptake and DNA-induced activation were strongly correlated ($R^2 = 0.762$, $p < 0.001$), indicating that the enhanced uptake of DNA is a crucial step in enhancing the DNA-induced activation. In addition, this led to the identification of a core sequence (C7-21*), which appeared critical in enhancing DNA uptake and activation. Interestingly, although the C1-15* fragment is unable to enhance DNA uptake or DNA-induced activation of HD11 cells, ITC analysis indicates it still has a high binding affinity for DNA (K_d = 22 nM; Supplemental Fig. 1E), suggesting that complex formation between the anionic DNA and a cationic peptide alone is not sufficient to enhance DNA uptake and DNA-induced macrophage activation.

CATH-2 enhances endosomal activation of TLR21

To determine whether DNA–CATH-2 complexes are actively internalized, we determined internalization of DNA-AF488 at 4°C. This reduced fluorescence back to background levels (Supple-

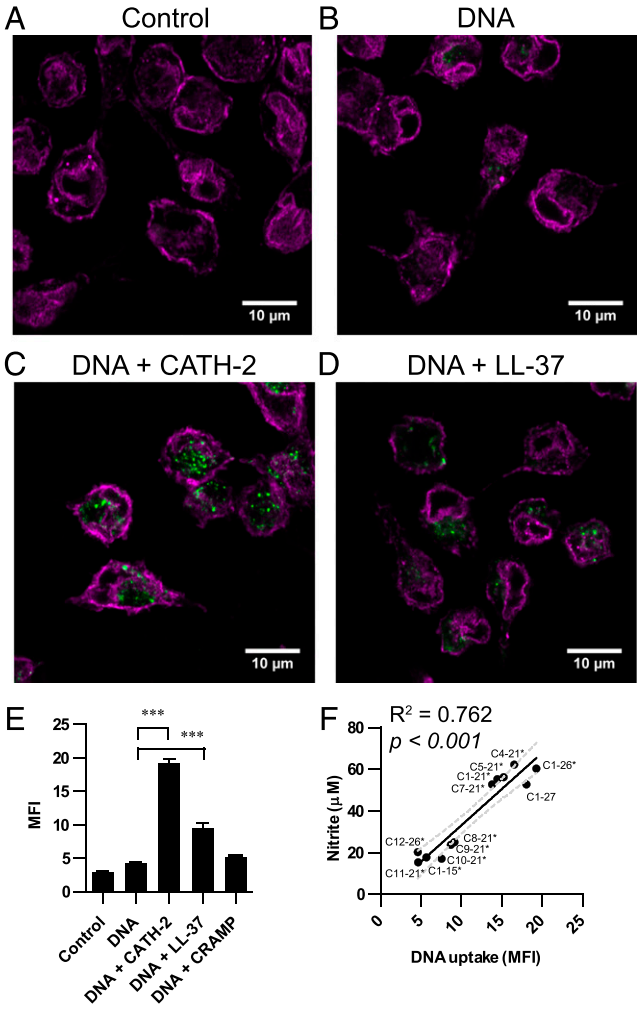

FIGURE 3. Localization and quantification of uptake of DNA-AF488 in macrophages. Confocal images of 4% paraformaldehyde-fixed HD11 cells, either (**A**) unstimulated or stimulated with 25 nM DNA-AF488 (green) and (**B**) no peptide, (**C**) CATH-2 (5 μM), or (**D**) LL-37 (5 μM). Membrane staining was performed by WGA-Alexa Fluor-647 (magenta). Images are representative of three independent experiments. (**E**) Quantification of DNA-AF488 (2.5 nM) uptake in HD11 cells after 4 h in the presence of different cathelicidins (5 μM) by flow cytometry. The *p* values are obtained by one-way ANOVA with Dunnett's post hoc test (***$p < 0.001$). $n = 3$–4. Error bars = SEM. (**F**) Quantification of NO production and DNA-AF488 uptake in HD11 cells. Cells are stimulated with 2.5 nM DNA-AF488 and different CATH-2 analogs (5 μM; Table I). Uptake is determined by flow cytometry. Correlation was determined by Pearson's correlation test. Graph shows averages of measured values and a best fit with 95% CI. $n = 3$.

mental Fig. 2A), indicating that the complex is actively internalized. To identify whether CATH-2 changed the pathway through which DNA was internalized, we stimulated HD11 cells with several endocytosis inhibitors (Fig. 4A). Uptake of both DNA alone and DNA in complex with CATH-2 was inhibited by chlorpromazine (clathrin-dependent uptake) and EIPA (micropinocytosis), indicating that the endocytic pathways involved in DNA uptake are similar in the presence and absence of CATH-2. In addition, both inhibitors also inhibited *IL1β* expression after stimulation with DNA alone or in complex with CATH-2 (Supplemental Fig. 2B). Analysis of inhibitor toxicity by WST-1 showed no toxic effects at the concentrations used (Supplemental Fig. 2C).

Activation of chicken macrophages by endocytosed DNA occurs through activation of the endosomal located TLR21, which acts as a functional homolog of the mammalian TLR9 (27). To date, this

Table I. Sequences of truncated CATH-2 peptides

C1-27	RFGRFLRKIRRFRPKVTITIQGSARFG
C1-26* (CATH-2)	RFGRFLRKIRRFRPKVTITIQGSARF-NH2
C1-15*	RFGRFLRKIRRFRPK-NH2
C12-26*	FRPKVTITIQGSARF-NH2
C1-21*	RFGRFLRKIRRFRPKVTITIQ-NH2
C4-21*	RFLRKIRRFRPKVTITIQ-NH2
C5-21*	FLRKIRRFRPKVTITIQ-NH2
C7-21*	RKIRRFRPKVTITIQ-NH2
C8-21*	KIRRFRPKVTITIQ-NH2
C9-21*	IRRFRPKVTITIQ-NH2
C10-21*	RRFRPKVTITIQ-NH2
C11-21*	RFRPKVTITIQ-NH2

has been the only DNA receptor identified in chickens. Activation of both TLR9 and TLR21 depends on endosomal acidification, which is thought to be necessary for proper cleavage of the receptor. To determine whether the DNA–CATH-2 complex could still activate the endosomal TLR21, we used bafilomycin A1 (Fig. 4B), NH_4Cl, or chloroquine (Supplemental Fig. 2D, 2E) to inhibit the endosomal acidification. This resulted in inhibition of HD11 activation by both DNA alone or in complex with CATH-2, indicating activation is TLR21 dependent. In contrast, activation of TLR4 on the cell surface by LPS was unaffected by the inhibition of endosomal acidification. In line with these results, inhibition of TLR21 activation by preincubation with an inhibitory ODN also reduced activation by both DNA and DNA–CATH-2 stimulation, while not affecting LPS-induced activation (Fig. 4C). A control ODN, which neither activates nor inhibits TLR21 activation, did not affect DNA-induced activation in the presence or absence of CATH-2. Together, these results indicate TLR21-dependent activation of HD11 cells by DNA–CATH-2 complexes.

Degradation of CATH-2 is essential for macrophage activation by DNA

Although the activation of the HD11 cells is enhanced by increasing DNA uptake because of complex formation with CATH-2, it is interesting to note that this complex formation is not hindering the interaction between DNA and the TLR21. This also appears to be the case in other studies investigating the role of HDPs on TLR9 activation (18, 28, 29). Nevertheless, very little is known about the intracellular stability of HDP–DNA complexes and how this influences endosomal TLR activation. To determine the stability of DNA–CATH-2-complexes in the endosomal environment, we determined binding affinity between CATH-2 and DNA by ITC analysis at pH 4.4 (Supplemental Fig. 2F). Although a difference in affinity was detected between pH 7.4 (11 nM) and pH 4.4 (32 nM), the acidic endosomal environment itself appears to be insufficient to destabilize the DNA–CATH-2 complex. A process that accompanies the decrease in endosomal pH is the activation of endosomal proteases. To test whether proteolytic breakdown of CATH-2 plays a role in induction of TLR21 activation, we compared CATH-2 activity to a proteolytic-resistant full D-amino acid analog of CATH-2. Intracellular DNA localization (Fig. 5A), as well as quantity of DNA uptake (Fig. 5B) in HD11 cells, was similar between CATH-2 and D-CATH-2. In addition, binding affinity between D-CATH-2 and DNA (11 nM; Supplemental Fig. 2G) was comparable between D-CATH-2 and the natural CATH-2. However, DNA-induced activation of HD11 cells as measured by NO production (Fig. 5C) or *IL1B* expression (Supplemental Fig. 2H) was completely inhibited in the presence of D-CATH-2, indicating that peptide degradation is critical for TLR21 activation. To determine whether D-CATH-2, but not CATH-2, remained in complex with the intracellular DNA, both D-CATH-2 and CATH-2 were synthesized with an N-terminal Dabcyl-label, which is able

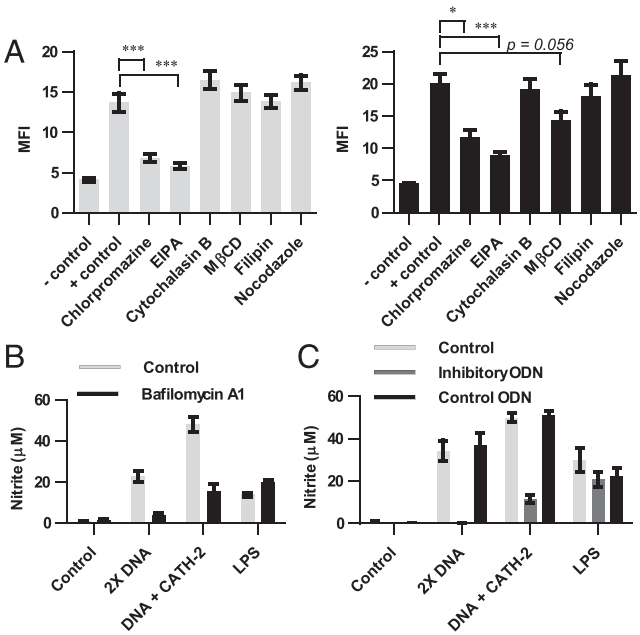

FIGURE 4. Endocytosis pathways involved in DNA uptake and TLR21 dependency of CATH-2 enhancement of DNA-induced activation. (**A**) Quantification of DNA-AF488 uptake in HD11 cells in the absence (*left panel*) or presence (*right panel*) of CATH-2 (5 μM) and different endocytosis inhibitors. Fluorescence was analyzed by flow cytometry after 4 h. Stimulation with DNA alone was performed with 10 nM DNA-AF488, whereas stimulation with DNA and CATH-2 was performed with 2.5 nM DNA-AF488. The *p* values are obtained by one-way ANOVA with Dunnett's post hoc test (*$p < 0.05$, ***$p < 0.001$). n = 4–6. Error bars = SEM. (**B** and **C**) NO production of HD11 cells after stimulation with 5 nM ODN-2006, 2.5 nM ODN-2006 + 5 μM CATH-2 or LPS (100 ng/ml) in combination with (B) bafilomycin A1 (250 nM), or (C) after preincubation with 2 μM inhibitor or control ODN. n = 3–5. Error bars = SEM.

to quench AF488 fluorescence. This means that close interaction between DNA-AF488 and Dabcyl-CATH-2 would lead to a loss of intracellular fluorescence. The N-terminal-Dabcyl group did not affect the activity of either CATH-2 or D-CATH-2 to alter DNA-induced activation (Fig. 5D). When measuring intracellular fluorescence by flow cytometry, coincubation with DNA and Dabcyl-D-CATH-2 resulted in a complete loss of fluorescence, in contrast to stimulation with DNA and Dabcyl-CATH-2, which showed similar intracellular fluorescence, compared with the unlabeled CATH-2 (Fig. 5E).

To further verify the endosomal degradation of CATH-2, we used endosomal acidification inhibitors to inhibit Dabcyl-CATH-2 degradation, which should result in a loss of intracellular fluorescence (Fig. 5F). Indeed, addition of bafilomycin A1 or NH_4Cl for 4 h resulted in low levels of intracellular AF488 fluorescence. Subsequent washing, removing the inhibitors and extracellular labeled DNA–peptide complexes, resulted in a time-dependent increase in intracellular fluorescence, that is, the presence of free labeled DNA in the acidified endosomes. Similar experiments with the Dabcyl-D-CATH-2 did not show an increase in fluorescence due to remaining quenching of the DNA-AF488 by the protease-resistant peptide. Taken together, these results show the importance of CATH-2 degradation from the CATH-2–DNA complex to activate the TLR21 and enhance macrophage activation (Fig. 6).

Discussion

HDPs have been shown to be multifunctional in their regulation of inflammatory responses. One of their previously described functions is the enhancement of DNA-induced IFN-α production in pDCs (18, 29). To our knowledge, this study is the first description of enhancement of DNA-induced immune activation by cathelicidins in a nonmammalian species. In addition, to our knowledge, we provide the first evidence for the necessity of intracellular cathelicidin degradation for endosomal TLR activation.

Our results show that cathelicidins of various species can enhance the immunogenicity of DNA by increasing the DNA uptake in chicken macrophages. This enhanced response against DNA–HDP complexes has also been reported for other mammalian cell types, such as pDCs, B cells, and monocytes (18, 25, 29–31), but appears to be limited to professional phagocytes. Keratinocyte responses toward DNA are even inhibited when DNA is presented in complex with LL-37 (32, 33). Of the previously described responses, macrophage activation by DNA–CATH-2 complexes appears to be most similar to B cell activation by DNA–LL-37 complexes (30), which also respond by upregulation of proinflammatory cytokines, such as IL-6, whereas reported responses of monocytes and pDCs are limited to enhanced type I IFN production (18, 25, 31), which was unaffected in our study. Interestingly, although many cathelicidins were able to enhance DNA-induced activation in chicken macrophages, increasing DNA uptake might not be the only way by which they can enhance endosomal TLR activation (34, 35).

In mammalian models, cellular activation in response to DNA–HDP complexes has so far been attributed to either activation of a TLR9-independent pathway, such as the activation of a cytosolic receptor in monocytes (31), or alternative downstream signaling of TLR9, leading to IRF7-phosphorylation and IFN-α production instead of NF-κB phosphorylation and proinflammatory cytokine production (18, 25, 28). In chickens, comparatively little is known yet about cellular responses toward DNA. So far, no cytosolic DNA receptors have been identified, and research on the downstream signaling of the TLR21 is limited to activation of NF-κB (27, 36). It will therefore be interesting to see whether TLR21 signaling is limited to NF-κB activation, or whether, like mammalian TLR9, alternative downstream pathways can be activated. Nevertheless, the increased proinflammatory response toward DNA–CATH-2 complexes observed in this study was induced in both chicken and mouse macrophages, suggesting that, regardless of alternative downstream pathways for TLR9 and possibly TLR21, macrophages of both species appear to respond in a NF-κB–dependent manner when presented with DNA–CATH-2 complexes. Further research will be needed to ascertain whether the different responses between cell types are due to differences in endosomal processing (37), downstream TLR signaling (38), or other processes.

Although the immunogenic capacity of DNA–HDP complexes is well established, little is known about the intracellular fate of these complexes. This study shows that once endocytosed, proteolytic breakdown of CATH-2 from its complex with DNA is essential for the DNA to be able to interact with the TLR21 and induce macrophage activation. However, studies on other endosomal TLRs and their ligands show the potential importance of endosomal degradation of cathelicidins. A recent report on activation of TLR3 by RNA–LL-37 complexes in epithelial cells indicated that interaction between LL-37 and RNA was lost during endosomal acidification (39). Although the stability of LL-37–RNA complexes at low pH are unclear (39, 40), proteolytic breakdown could be the reason for the loss of RNA–LL-37 interaction and increased TLR3 activation. In addition, increased LPS uptake was detected in epithelial cells in the presence of LL-37 (41). This, in turn, led to an increase of intracellular TLR4 activation. Although LL-37 normally inhibits LPS-induced TLR4

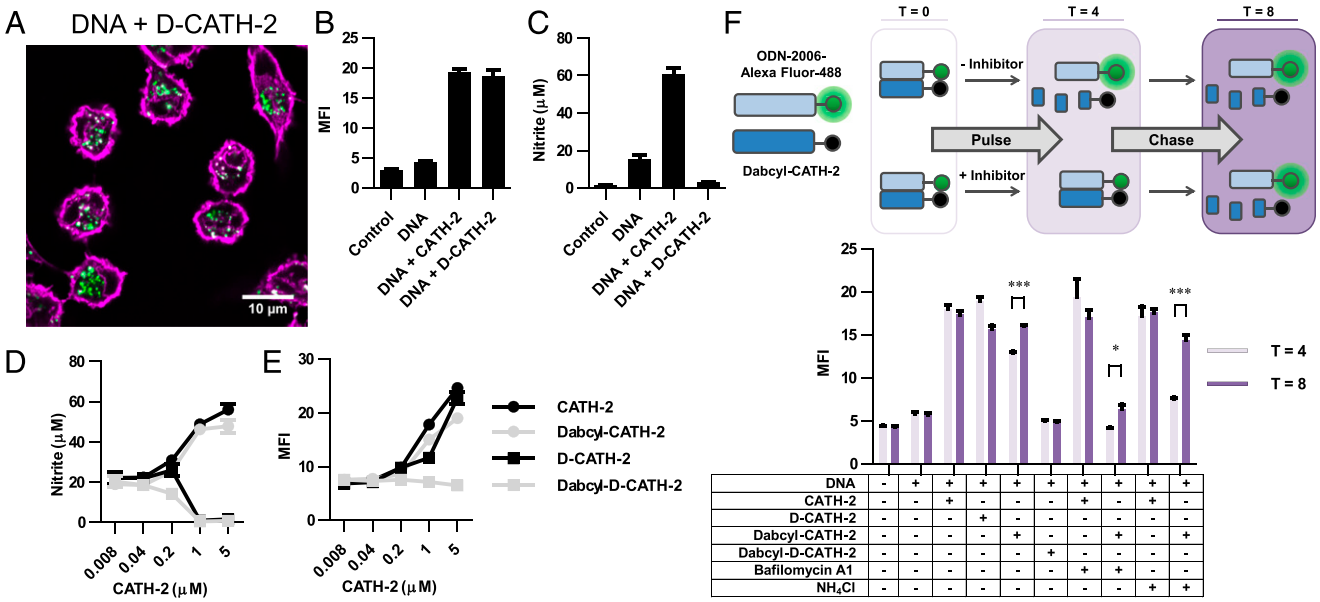

FIGURE 5. CATH-2 degradation in endosomal compartments of macrophages. (**A**) Confocal imaging of HD11 cells fixed with 4% paraformaldehyde after stimulation with 25 nM DNA-AF488 (green) and D-CATH-2 (5 µM). Membranes stained with WGA-647 (magenta). Shown is a representative image of three independent experiments. (**B** and **C**) Quantification of (B) DNA uptake and (C) NO production after stimulation of HD11 cells with 2.5 nM DNA-AF488 in the presence of 5 µM CATH-2 or D-CATH-2. $n = 3$. Error bars = SEM. (**D**) NO production by HD11 cells after stimulation with DNA-AF488 (2.5 nM) in the presence of several concentrations of CATH-2 or D-CATH-2 with or without a Dabcyl-label. $n = 3$. Error bars = SEM. (**E**) Quantification of intracellular fluorescence in HD11 cells by flow cytometry after stimulation with DNA-AF488 (2.5 nM) in the presence of several concentrations of CATH-2 or D-CATH-2 with or without a Dabcyl-label. $n = 4$–5. Error bars = SEM. (**F**) Endosomal CATH-2 degradation over time. HD11 cells are stimulated for 4 h (T = 4) with DNA-AF488 (2.5 nM), Dabcyl-labeled or unlabeled CATH-2 (5 µM), and with or without acidification inhibitor (bafilomycin A1 or NH_4Cl). After 4 h cells are washed and incubated for an additional 4 h (T = 8). Flow-cytometric analysis of intracellular fluorescence is determined at T = 4 and T = 8. The p values are obtained by one-sided independent sample t tests (*$p < 0.05$, ***$p < 0.001$). $n = 4$. Error bars = SEM.

activation at the cell surface, it is very well possible that because of endosomal LL-37 degradation, LPS is released from a complex with LL-37, which enables it to activate TLR4 inside endosomes.

The elucidation of cathelicidin functions in TLR activation in vitro has revealed a number of potential functions for cathelicidins during infections. In addition, animal studies have provided evidence for these functions in vivo as well. Interestingly, although most of these studies have been focusing on the strong activation of pDCs by DNA–HDP-complexes, experiments have demonstrated that not only IFN-α, but also other proinflammatory cytokines are upregulated in vivo after stimulation with DNA–HDP-complexes (29, 42). The in vitro proinflammatory macrophage responses described in this article could play a role in the production of proinflammatory cytokines in in vivo models as well.

Although interesting from a biological point of view, functions like the enhancement of DNA-induced activation can prove useful in HDP-based anti-infective therapies as well. In fact, HDP-based peptides have been shown to enhance vaccination efficiency in several in vivo models, in which the vaccination mixture contains synthetic DNA (43–47). Although little is known about the effects of these specific HDPs on DNA-induced immune activation, it is possible that part of their efficacy comes from increasing the proinflammatory DNA-induced immune response. Moreover, therapeutic use of HDPs as antimicrobials could affect inflammatory responses because of the abundant sources of extracellular DNA during infections and inflammation (11, 12). These inflammatory responses can be adjusted through peptide modifications to improve vaccination efficacy.

In conclusion, this study provides a detailed analysis of the mechanism by which cathelicidins enhance DNA-induced macrophage activation in chickens, but also mammalian macrophages. We show that DNA and cathelicidins form a complex, which leads to enhanced endocytosis of the DNA. After endocytosis, proteases in the acidified endosome degrade cathelicidin from the complex, which is needed to liberate the DNA and allow for interaction between the DNA and TLR21 (Fig. 6). These results help in better understanding the role of cathelicidins in chicken innate host defense but also give a possible explanation for the beneficial effects of HDPs in vaccinations and potential immunoregulatory effects of other HDP-based anti-infective therapies.

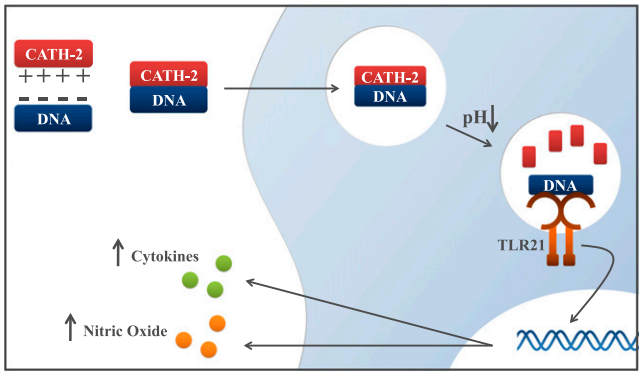

FIGURE 6. Model for regulatory role of CATH-2 in DNA-induced macrophage activation. Extracellular binding of DNA to CATH-2 due to ionic interaction promotes the uptake of DNA in endosomal compartments, which is followed by endosomal acidification, resulting in protease activation and subsequent CATH-2 degradation. After CATH-2 degradation, DNA is free to bind the TLR21, resulting in enhanced NO production and cytokine gene expression.

Acknowledgments

We thank Marloes Hoeksema for technical support in ELISA experiments performed on RAW 264.7 cells.

Disclosures

The authors have no financial conflicts of interest.

References

1. Cuperus, T., M. Coorens, A. van Dijk, and H. P. Haagsman. 2013. Avian host defense peptides. *Dev. Comp. Immunol.* 41: 352–369.
2. Wassing, G. M., P. Bergman, L. Lindbom, and A. M. van der Does. 2015. Complexity of antimicrobial peptide regulation during pathogen-host interactions. *Int. J. Antimicrob. Agents* 45: 447–454.
3. Hilchie, A. L., K. Wuerth, and R. E. Hancock. 2013. Immune modulation by multifaceted cationic host defense (antimicrobial) peptides. *Nat. Chem. Biol.* 9: 761–768.
4. Chromek, M., Z. Slamová, P. Bergman, L. Kovács, L. Podracká, I. Ehrén, T. Hökfelt, G. H. Gudmundsson, R. L. Gallo, B. Agerberth, and A. Brauner. 2006. The antimicrobial peptide cathelicidin protects the urinary tract against invasive bacterial infection. *Nat. Med.* 12: 636–641.
5. Chromek, M., I. Arvidsson, and D. Karpman. 2012. The antimicrobial peptide cathelicidin protects mice from *Escherichia coli* O157:H7-mediated disease. *PLoS One* 7: e46476.
6. Nizet, V., T. Ohtake, X. Lauth, J. Trowbridge, J. Rudisill, R. A. Dorschner, V. Pestonjamasp, J. Piraino, K. Huttner, and R. L. Gallo. 2001. Innate antimicrobial peptide protects the skin from invasive bacterial infection. *Nature* 414: 454–457.
7. Benincasa, M., C. Pelillo, S. Zorzet, C. Garrovo, S. Biffi, R. Gennaro, and M. Scocchi. 2010. The proline-rich peptide Bac7(1-35) reduces mortality from *Salmonella typhimurium* in a mouse model of infection. *BMC Microbiol.* 10: 178.
8. Rivas-Santiago, B., J. E. Castañeda-Delgado, C. E. Rivas Santiago, M. Waldbrook, I. González-Curiel, J. C. León-Contreras, J. A. Enciso-Moreno, V. del Villar, J. Mendez-Ramos, R. E. Hancock, and R. Hernandez-Pando. 2013. Ability of innate defence regulator peptides IDR-1002, IDR-HH2 and IDR-1018 to protect against *Mycobacterium tuberculosis* infections in animal models. *PLoS One* 8: e59119.
9. Bommineni, Y. R., G. H. Pham, L. T. Sunkara, M. Achanta, and G. Zhang. 2014. Immune regulatory activities of fowlicidin-1, a cathelicidin host defense peptide. *Mol. Immunol.* 59: 55–63.
10. Yount, N. Y., and M. R. Yeaman. 2012. Emerging themes and therapeutic prospects for anti-infective peptides. *Annu. Rev. Pharmacol. Toxicol.* 52: 337–360.
11. Pisetsky, D. S. 2012. The origin and properties of extracellular DNA: from PAMP to DAMP. *Clin. Immunol.* 144: 32–40.
12. Bayles, K. W. 2007. The biological role of death and lysis in biofilm development. *Nat. Rev. Microbiol.* 5: 721–726.
13. Friedlander, A. M. 1975. DNA release as a direct measure of microbial killing. I. Serum bactericidal activity. *J. Immunol.* 115: 1404–1408.
14. Kaplan, J. B., E. A. Izano, P. Gopal, M. T. Karwacki, S. Kim, J. L. Bose, K. W. Bayles, and A. R. Horswill. 2012. Low levels of β-lactam antibiotics induce extracellular DNA release and biofilm formation in Staphylococcus aureus. *MBio* 3: e00198–e12.
15. Kaplan, M. J., and M. Radic. 2012. Neutrophil extracellular traps: double-edged swords of innate immunity. *J. Immunol.* 189: 2689–2695.
16. Kono, H., and K. L. Rock. 2008. How dying cells alert the immune system to danger. *Nat. Rev. Immunol.* 8: 279–289.
17. Scheiermann, J., and D. M. Klinman. 2014. Clinical evaluation of CpG oligonucleotides as adjuvants for vaccines targeting infectious diseases and cancer. *Vaccine* 32: 6377–6389.
18. Lande, R., J. Gregorio, V. Facchinetti, B. Chatterjee, Y. H. Wang, B. Homey, W. Cao, Y. H. Wang, B. Su, F. O. Nestle, et al. 2007. Plasmacytoid dendritic cells sense self-DNA coupled with antimicrobial peptide. *Nature* 449: 564–569.
19. Lande, R., D. Ganguly, V. Facchinetti, L. Frasca, C. Conrad, J. Gregorio, S. Meller, G. Chamilos, R. Sebasigari, V. Riccieri, et al. 2011. Neutrophils activate plasmacytoid dendritic cells by releasing self-DNA-peptide complexes in systemic lupus erythematosus. *Sci. Transl. Med.* 3: 73ra19.
20. Diana, J., Y. Simoni, L. Furio, L. Beaudoin, B. Agerberth, F. Barrat, and A. Lehuen. 2013. Crosstalk between neutrophils, B-1a cells and plasmacytoid dendritic cells initiates autoimmune diabetes. *Nat. Med.* 19: 65–73.
21. van Dijk, A., E. J. Veldhuizen, A. J. van Asten, and H. P. Haagsman. 2005. CMAP27, a novel chicken cathelicidin-like antimicrobial protein. *Vet. Immunol. Immunopathol.* 106: 321–327.
22. Beug, H., A. von Kirchbach, G. Döderlein, J. F. Conscience, and T. Graf. 1979. Chicken hematopoietic cells transformed by seven strains of defective avian leukemia viruses display three distinct phenotypes of differentiation. *Cell* 18: 375–390.
23. Qureshi, M. A., L. Miller, H. S. Lillehoj, and M. D. Ficken. 1990. Establishment and characterization of a chicken mononuclear cell line. *Vet. Immunol. Immunopathol.* 26: 237–250.
24. Raschke, W. C., S. Baird, P. Ralph, and I. Nakoinz. 1978. Functional macrophage cell lines transformed by Abelson leukemia virus. *Cell* 15: 261–267.
25. Baumann, A., T. Démoulins, S. Python, and A. Summerfield. 2014. Porcine cathelicidins efficiently complex and deliver nucleic acids to plasmacytoid dendritic cells and can thereby mediate bacteria-induced IFN-α responses. *J. Immunol.* 193: 364–371.
26. Hanagata, N. 2012. Structure-dependent immunostimulatory effect of CpG oligodeoxynucleotides and their delivery system. *Int. J. Nanomedicine* 7: 2181–2195.
27. Keestra, A. M., M. R. de Zoete, L. I. Bouwman, and J. P. van Putten. 2010. Chicken TLR21 is an innate CpG DNA receptor distinct from mammalian TLR9. *J. Immunol.* 185: 460–467.
28. Coch, C., N. Busch, V. Wimmenauer, E. Hartmann, M. Janke, M. M. Abdel-Mottaleb, A. Lamprecht, J. Ludwig, W. Barchet, M. Schlee, and G. Hartmann. 2009. Higher activation of TLR9 in plasmacytoid dendritic cells by microbial DNA compared with self-DNA based on CpG-specific recognition of phosphodiester DNA. *J. Leukoc. Biol.* 86: 663–670.
29. Tewary, P., G. de la Rosa, N. Sharma, L. G. Rodriguez, S. G. Tarasov, O. M. Howard, H. Shirota, F. Steinhagen, D. M. Klinman, D. Yang, and J. J. Oppenheim. 2013. β-Defensin 2 and 3 promote the uptake of self or CpG DNA, enhance IFN-α production by human plasmacytoid dendritic cells, and promote inflammation. *J. Immunol.* 191: 865–874.
30. Hurtado, P., and C. A. Peh. 2010. LL-37 promotes rapid sensing of CpG oligodeoxynucleotides by B lymphocytes and plasmacytoid dendritic cells. *J. Immunol.* 184: 1425–1435.
31. Chamilos, G., J. Gregorio, S. Meller, R. Lande, D. P. Kontoyiannis, R. L. Modlin, and M. Gilliet. 2012. Cytosolic sensing of extracellular self-DNA transported into monocytes by the antimicrobial peptide LL37. *Blood* 120: 3699–3707.
32. Dombrowski, Y., M. Peric, S. Koglin, C. Kammerbauer, C. Göss, D. Anz, M. Simanski, R. Gläser, J. Harder, V. Hornung, et al. 2011. Cytosolic DNA triggers inflammasome activation in keratinocytes in psoriatic lesions. *Sci. Transl. Med.* 3: 82ra38.
33. Morizane, S., K. Yamasaki, B. Mühleisen, P. F. Kotol, M. Murakami, Y. Aoyama, K. Iwatsuki, T. Hata, and R. L. Gallo. 2012. Cathelicidin antimicrobial peptide LL-37 in psoriasis enables keratinocyte reactivity against TLR9 ligands. *J. Invest. Dermatol.* 132: 135–143.
34. Nakagawa, Y., and R. L. Gallo. 2015. Endogenous intracellular cathelicidin enhances TLR9 activation in dendritic cells and macrophages. *J. Immunol.* 194: 1274–1284.
35. Schmidt, N. W., F. Jin, R. Lande, T. Curk, W. Xian, C. Lee, L. Frasca, D. Frenkel, J. Dobnikar, M. Gilliet, and G. C. Wong. 2015. Liquid-crystalline ordering of antimicrobial peptide-DNA complexes controls TLR9 activation. *Nat. Mater.* 14: 696–700.
36. Ciraci, C., and S. J. Lamont. 2011. Avian-specific TLRs and downstream effector responses to CpG-induction in chicken macrophages. *Dev. Comp. Immunol.* 35: 392–398.
37. de Geus, E. D., C. A. Jansen, and L. Vervelde. 2012. Uptake of particulate antigens in a nonmammalian lung: phenotypic and functional characterization of avian respiratory phagocytes using bacterial or viral antigens. *J. Immunol.* 188: 4516–4526.
38. Gilliet, M., W. Cao, and Y. J. Liu. 2008. Plasmacytoid dendritic cells: sensing nucleic acids in viral infection and autoimmune diseases. *Nat. Rev. Immunol.* 8: 594–606.
39. Singh, D., R. Vaughan, and C. C. Kao. 2014. LL-37 peptide enhancement of signal transduction by Toll-like receptor 3 is regulated by pH: identification of a peptide antagonist of LL-37. *J. Biol. Chem.* 289: 27614–27624.
40. Hasan, M., C. Rukšznis, Y. Wang, and C. A. Leifer. 2011. Antimicrobial peptides inhibit polyinosinic-polycytidylic acid-induced immune responses. *J. Immunol.* 187: 5653–5659.
41. Shaykhiev, R., J. Sierigk, C. Herr, G. Krasteva, W. Kummer, and R. Bals. 2010. The antimicrobial peptide cathelicidin enhances activation of lung epithelial cells by LPS. *FASEB J.* 24: 4756–4766.
42. Gregorio, J., S. Meller, C. Conrad, A. Di Nardo, B. Homey, A. Lauerma, N. Arai, R. L. Gallo, J. Digiovanni, and M. Gilliet. 2010. Plasmacytoid dendritic cells sense skin injury and promote wound healing through type I interferons. *J. Exp. Med.* 207: 2921–2930.
43. Kovacs-Nolan, J., J. W. Mapletoft, L. Latimer, L. A. Babiuk, and Sv. Hurk. 2009. CpG oligonucleotide, host defense peptide and polyphosphazene act synergistically, inducing long-lasting, balanced immune responses in cattle. *Vaccine* 27: 2048–2054.
44. Kovacs-Nolan, J., J. W. Mapletoft, Z. Lawman, L. A. Babiuk, and S. van Drunen Littel-van den Hurk. 2009. Formulation of bovine respiratory syncytial virus fusion protein with CpG oligodeoxynucleotide, cationic host defence peptide and polyphosphazene enhances humoral and cellular responses and induces a protective type 1 immune response in mice. *J. Gen. Virol.* 90: 1892–1905.
45. Kovacs-Nolan, J., L. Latimer, A. Landi, H. Jenssen, R. E. Hancock, L. A. Babiuk, and S. van Drunen Littel-van den Hurk. 2009. The novel adjuvant combination of CpG ODN, indolicidin and polyphosphazene induces potent antibody- and cell-mediated immune responses in mice. *Vaccine* 27: 2055–2064.
46. Kindrachuk, J., H. Jenssen, M. Elliott, R. Townsend, A. Nijnik, S. F. Lee, V. Gerdts, L. A. Babiuk, S. A. Halperin, and R. E. Hancock. 2009. A novel vaccine adjuvant comprised of a synthetic innate defence regulator peptide and CpG oligonucleotide links innate and adaptive immunity. *Vaccine* 27: 4662–4671.
47. Garlapati, S., N. F. Eng, T. G. Kiros, J. Kindrachuk, G. K. Mutwiri, R. E. Hancock, S. A. Halperin, A. A. Potter, L. A. Babiuk, and V. Gerdts. 2011. Immunization with PCEP microparticles containing pertussis toxoid, CpG ODN and a synthetic innate defense regulator peptide induces protective immunity against pertussis. *Vaccine* 29: 6540–6548.